Electric Field and Strain-Induced Transformation of Magnetic Skyrmion in a Chiral Multiferroic Cu_2OSeO_3

We have investigated electric-field-induced magnetic phase transition between the skyrmion lattice and the helix, and the emergence of the chiral soliton lattice by uniaxial strain in the multiferroic chiral magnet Cu_2OSeO_3 by means of small-angle soft X-ray scattering at the Cu L_3 absorption edge. By application of an electric field, the skyrmion lattice transforms into helices with distinct modulation vectors depending on the sign of the electric field. On the other hand, the tensile strain stabilizes a helical spin structure with the modulation vector along the strain direction. When the field perpendicular to the modulation vector is increased, large shrinkage occurs and higher-order diffraction peaks are also observed, which is in accordance with a typical feature of the chiral soliton lattice.

Long after the first theoretical prediction of skyrmions in magnetic systems in the 1980s [1], skyrmions forming triangular lattices have been experimentally discovered in B20-type cubic chiral helimagnets [2–4]. Owing to their topological stability, nanometric size (2–200 nm), formation even above room temperature, and versatile electromagnetic responses, skyrmions are promising candidates for spintronic applications and have attracted extensive experimental and theoretical studies. In particular, the creation and annihilation of skyrmions is an indispensable function for device applications and hence an important subject of research. One established way is to control magnetic anisotropy by applying external fields: transformation between the skyrmion and conical spin structure, i.e., a helix with the ferromagnetic moment along the magnetic-field direction, has been demonstrated by application of hydrostatic pressure, uniaxial pressure, and electric fields in bulk samples of cubic chiral helimagnets.

In this study we investigated electric-field-induced phase transition and tensile strain effect in a thin plate of Cu_2OSeO_3 by means of small-angle resonant soft X-ray scattering (RSXS) measurement. A single crystal of Cu_2OSeO_3 was grown by the chemical vapor transport method. Small-angle RSXS measurement was performed at the soft X-ray beamline BL-16A. We used circularly polarized X-ray and the RSXS was recorded using a direct-detection CCD camera. Since the attenuation length at the Cu L_3 edge (~931 eV) is less than 200 nm, to optimize transmission and diffraction intensity, a thin plate of Cu_2OSeO_3 with a thickness of about 200 nm was fabricated by using the focused ion beam (FIB) technique. The backside of the SiN membrane window was covered with gold film, and a pinhole of ~7 μm in diameter was drilled. The sample was mounted to cover the pinhole and affixed with tungsten contacts on gold electrodes in order to apply the electric field [Fig. 1(a)]. We applied a voltage of up to ±150 V between two tungsten electrodes a distance of ~100 μm apart and estimated the magnitude of the electric field by considering this distance. A magnetic field of up to 0.5 T was applied by using a Helmholtz coil along the normal of the plate.

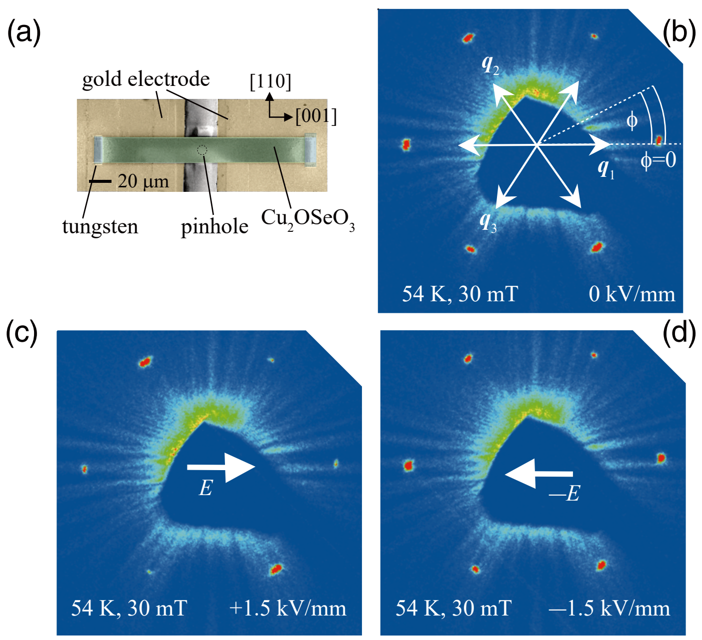

Figure 1: (a) A picture of the thin plate of Cu_2OSeO_3 fabricated by a focused ion beam thinning technique. Diffraction patterns at 54 K and 30 mT under (b) E = 0 kV/mm, (c) +1.5 kV/mm, and (d) −1.5 kV/mm.

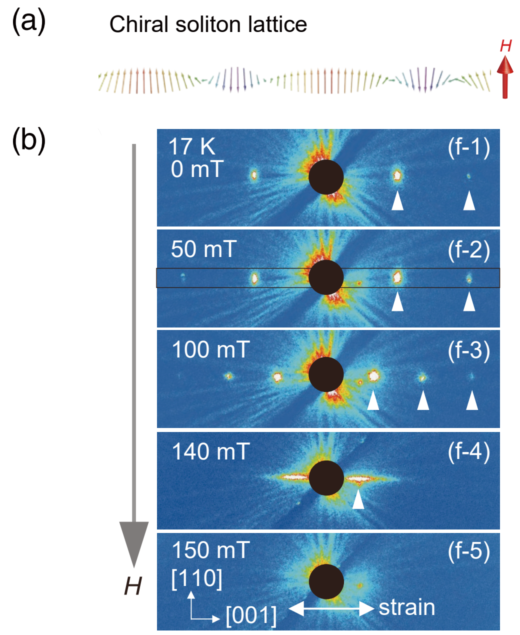

Figure 2: (a) Schematic illustrations of the chiral soliton lattice, and (b) the magnetic-field variation of the diffraction patterns at 17 K in the strained sample. Diffraction spots existing on the right side are highlighted by white arrows.

Figures 1(b)–(d) show typical diffraction patterns of the skyrmion lattice under zero, positive, and negative electric field, respectively. The diffraction intensity arising from the skyrmion lattice is basically isotropic at E = 0 [Fig. 1(b)], whereas by applying a positive electric field, the diffraction intensity of q1 and q3 modulations almost disappear and the diffraction pattern becomes highly anisotropic [Fig. 1(c)]. At negative E, by contrast, the diffraction intensity of the q2 modulation is not so changed and those of the q1 and q3 modulations become stronger [Fig. 1(d)]. These asymmetric behaviors with respect to the sign of the electric field are distinct from those expected for bulk systems and also exclude spurious effects such as heating effect. The anisotropic diffraction intensity as observed in Figs. 1(c) and (d) can be elucidated by considering the electric field induced transformation from skyrmion lattice into the distinct helical magnetic structure depending on the sign of the electric field [6].

In addition, when the sample is fixed at both edges by electrodes, the difference in thermal expansion between the sample and the Si_3N_4 membrane produces tensile strain along the [001] axis which is of the order of hundreds of MPa. We revealed that the tensile strain would strongly stabilize the helical state up to higher fields at lower temperatures, and thus typical behaviors of the chiral soliton lattice (CSL) [Fig. 2 (a)] appear [7]. As shown in Fig. 2(b), the higher-order q diffraction peaks are clearly observed and |q| is reduced with increasing the magnetic field. The magnetic-field dependencies of the q vectors and the higher-order diffractions are in accordance with those of the CSL, whose magnetic field dependence can be theoretically derived by the analytical solution of the sine-Gordon equation [7].

REFERENCES

[1] A. N. Bogdanov and D. A. Yablonskii, *Sov. Phys. JETP* **68**, 101 (1989).
[2] S. Mühlbauer, B. Binz, F. Jonietz, C. Pfleiderer, A. Rosch, A. Neubauer, R. Georgii and P. Böni, *Science* **323**, 915 (2009).
[3] X. Z. Yu, Y. Onose, N. Kanazawa, J. H. Park, J. H. Han, Y. Matsui, N. Nagaosa and Y. Tokura, *Nature (London)* **465**, 901 (2010).
[4] S. Seki, X. Z. Yu, S. Ishiwata and Y. Tokura, *Science* **336**, 198 (2012).
[5] Y. Yamasaki, D. Morikawa, T. Honda, H. Nakao, Y. Murakami, N. Kanazawa, M. Kawasaki, T. Arima and Y. Tokura, *Phys. Rev. B* **92**, 220421 (2015).
[6] Y. Okamura, Y. Yamasaki, D. Morikawa, T. Honda, V. Ukleev, H. Nakao, Y. Murakami, K. Shibata, F. Kagawa, S. Seki, T. Arima and Y. Tokura, *Phys. Rev. B*, **95**, 184411 (2017).
[7] Y. Okamura, Y. Yamasaki, D. Morikawa, T. Honda, V. Ukleev, H. Nakao, Y. Murakami, K. Shibata, F. Kagawa, S. Seki, T. Arima and Y. Tokura, *Phys. Rev. B* **96**, 174417 (2017).

BEAMLINE

BL-16A

Y. Yamasaki (NIMS)